

Field-induced modification of the electronic structure in BTBT-based organic thin films observed by NEXAFS spectroscopy

Cite as: Appl. Phys. Lett. **121**, 183503 (2022); <https://doi.org/10.1063/5.0105893>

Submitted: 26 June 2022 • Accepted: 08 October 2022 • Published Online: 02 November 2022

 M. Johnson,  T. Hawly,  B. Zhao, et al.



View Online



Export Citation



CrossMark

ARTICLES YOU MAY BE INTERESTED IN

Lattice and electronic structure of ScN observed by angle-resolved photoemission spectroscopy measurements

Applied Physics Letters **121**, 182102 (2022); <https://doi.org/10.1063/5.0119628>

A simple structured solar selective absorber for application in thermoelectric energy harvesters

Applied Physics Letters **121**, 173906 (2022); <https://doi.org/10.1063/5.0116616>

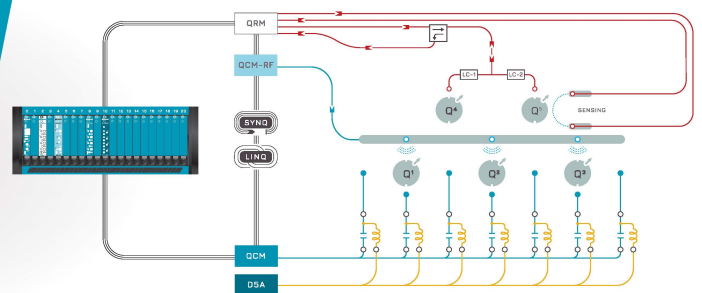
On-demand generation of optically active defects in monolayer WS₂ by a focused helium ion beam

Applied Physics Letters **121**, 183101 (2022); <https://doi.org/10.1063/5.0118697>

 QBLOX

Integrates all
Instrumentation + Software
for Control and Readout of
Spin Qubits

[visit our website >](#)



Field-induced modification of the electronic structure in BTBT-based organic thin films observed by NEXAFS spectroscopy

Cite as: Appl. Phys. Lett. **121**, 183503 (2022); doi: 10.1063/5.0105893

Submitted: 26 June 2022 · Accepted: 8 October 2022 ·

Published Online: 2 November 2022



View Online



Export Citation



CrossMark

M. Johnson,¹ T. Hawly,¹ B. Zhao,² M. Halik,² A. Nefedov,³ and R. Fink^{1,a)}

AFFILIATIONS

¹Department of Chemistry and Pharmacy, Friedrich-Alexander-Universität Erlangen-Nürnberg, Erlangen (FAU), Erlangen 91058, Germany

²Organic Materials and Devices (OMD), Friedrich-Alexander-Universität Erlangen-Nürnberg (FAU), Erlangen 91058, Germany

³Institute of Functional Interfaces (IFG), Karlsruhe Institute of Technology (KIT), Eggenstein-Leopoldshafen 76344, Germany

^{a)}Author to whom correspondence should be addressed: rainer.fink@fau.de

ABSTRACT

We present an *in operando* near-edge x-ray absorption fine structure (NEXAFS) study on p-type [11-(benzo[b]benzo[4,5]thieno[2,3-d]thiophen-2-yl)dodecyl] BTBT-based self-assembled monolayer (BTBT-SAM) films. As a 2D-model system, the BTBT-SAM offers direct insight into the active organic semiconductor layer without interfering bulk materials. This allows for the observation of polaronic states caused by charged species at the dielectric/organic interface. Linear NEXAFS dichroism is employed to derive the molecular orientation of the BTBT subunit. Field-induced modifications in the unoccupied molecular orbitals are observed in the NEXAFS spectra. The spectral changes in the on- and off-states are discussed in the context of polaron formation due to charge accumulation induced by the applied electric field.

Published under an exclusive license by AIP Publishing. <https://doi.org/10.1063/5.0105893>

The chemical versatility and compatibility in combination with cost-efficient solution-based processing techniques^{1–5} has made organic semiconductors promising candidates for new generation (opto-)electronic devices.⁶ Among those devices, organic field-effect transistors (OFETs) are particularly interesting since they can be used as basic switches in a broad range of electronic applications⁷ and function as excellent test objects for studying fundamental questions about the charge accumulation and transport mechanism in organic semiconductor materials.^{8–11} The majority of *in operando* studies in the literature that focus on the electronic structure modification inside the active layer of working OFETs are conducted using optical spectroscopy techniques. Their results clearly demonstrate the difference in the conventional band bending model used for inorganic materials as they revealed new electronic states in the bandgap, which is generated by field-induced charge carriers.^{12–14} In contrast, x-ray-based spectroscopic techniques offer additional experimental opportunities to explore the electronic structure within the active organic film due to their element specificity. While previously reported studies by Hub *et al.*,¹⁵ Kato *et al.*,¹⁶ and Nagamura *et al.*,¹⁷ demonstrated the general applicability of different x-ray based spectroscopic tools for *in operando* investigations, they did not reveal any variation in the electronic states in the valence region that

could unambiguously be attributed to charge injection. One straightforward reason is the extremely low concentration of charges present within the accumulation layer of an OFET structure (i.e., ~one unit charge per 1000 molecules),¹² which easily perishes in the background of absorption from bulk materials.

In conventional OFETs, charge transport takes place in the first few nanometers to the organic–dielectric interface.^{18,19} Therefore, the most affected regime is located right at the interface, which needs to be addressed for optimum detection of a potentially small effect. This implies that the device should operate at minimum film thickness, and in consequence, the optimum device is composed of just one monolayer in order to prevent absorption from uninfluenced bulk material. One category of specimens that satisfies this requirement is self-assembled monolayers (SAMs) since they form a dense and uniform single layer film, which is stabilized by covalent bonds to a crystalline solid substrate. The absence of bulk material makes them truly two-dimensional systems and allows direct access to the charge transporting layer. Due to major improvements in molecular design, SAMs have gone from pure surface modifiers to reliable organic semiconductors, and nowadays, a variety of SAMs has been successfully used as charge transporting layers in self-assembled monolayers field-effect transistors (SAMFETs).^{20–23}

In this study, we have used [11-(benzo[b]benzo[4,5]thieno[2,3-d]thiophen-2-yl)dodecyl]-phosphonic acid (BTBT-C11-PA) as an active layer material to reveal electronic modifications taking place inside the organic layer induced by an external electric field using near-edge x-ray absorption fine structure spectroscopy (NEXAFS). NEXAFS uses soft x rays to resonantly excite core electrons into unoccupied electronic states. Due to the photon energy dependent absorption, it enables elemental specific insight into the molecular electronic structure and may address specific atoms within the organic framework. Furthermore, at selected absorption resonances, the linear absorption dichroism can be used to deduce the average molecular orientation inside the analyzed sample.²⁴ The BTBT-SAM [Fig. 1(a)] is an excellent two-dimensional model system, which allows direct access to the conjugated core unit and has successfully been used in low-voltage, high mobility SAMFET devices.²⁵ A sketch of our simple OFET like device as well as the measurement setup is shown in Fig. 1(b). Heavily doped silicon wafers with a 5 nm native SiO₂ layer and a 20 nm thick atomic-layer deposition (ALD)-prepared aluminum oxide film were used as substrates. Subsequently, the BTBT-SAM layer was formed by immersing the substrate into a BTBT-phosphonic acid solution (0.05 mM) for 72 h.²⁵ Finally, 40 nm thick gold electrodes were deposited by Au evaporation from a resistively heated crucible. The Au coated contact was covered with a stainless-steel frame contact featuring a 5 × 10 mm² window.

To determine the overall SAM morphology and to study the gate voltage effect induced by the electrical field, C K-edge NEXAFS spectra were recorded at the HE-SGM beamline of the Bessy II synchrotron facility at the Helmholtz-Zentrum für Materialien und Energie (Berlin, Germany). The spectra were acquired with a high surface sensitivity using a channel-plate based partial electron yield detector as a high pass filter. The pass energy was adjusted according to the applied voltages to compensate for the kinetic energy of the secondary (Auger) electrons. To eliminate any possible influence of carbon contamination present in the optical elements of the beamline, all spectra were corrected using the transmission function measured by the gold mesh before the endstation. The absolute photon energy was calibrated using Highly-Oriented Pyrolytic Graphite (HOPG) as a reference, and all spectra were normalized to pre- (280 eV) and post-absorption edges

(325 eV) according to standard procedures.²⁴ In the present study, only carbon K-edge absorption was measured as the sulfur L- or K-edges are not accessible in the experimental setups available to us.

In Fig. 2(a), normalized C K-edge NEXAFS spectra of the BTBT-SAM for six different incidence angles θ are shown. The spectra exhibit the NEXAFS fingerprint typical for BTBT subunits with sharp peaks near 286 eV assigned to localized C1s $\rightarrow\pi^*$ (C=C) transitions of the aromatic BTBT core unit. Peaks in the region of the ionization edge around 289 eV are of hybrid nature as they arise from C1s $\rightarrow\sigma^*$ (C-H), C1s $\rightarrow\sigma^*$ (C-S), and C1s $\rightarrow\pi^*$ (C=C) transitions.^{26–28} The broad spectral features that are observed for photon energies above the ionization edge >293 eV are mainly attributed to C1s $\rightarrow\sigma^*$ (C-C, C=C) transitions of the aromatic core unit and alkyl chain.^{26,29} With varying incidence angle θ , we observe a strong change in the absorption intensity for both resonant C1s $\rightarrow\pi^*$ and C1s $\rightarrow\sigma^*$ transitions. At large photon incidence angles θ , the π^* -transitions are of highest intensity while the σ^* -transitions decrease in intensity with opposite behavior. These intensity variations are caused by the NEXAFS linear dichroism effect and allude to the preferential arrangement of the molecules inside the organic layer.²⁴

An expansion of the π^* -region for the normal incidence spectra ($\theta = 90^\circ$) is presented in Fig. 2(b). Aside from the intense C1s $\rightarrow\pi^*$ (C=C) resonances discussed at 285.7, 286.1, and 286.3 eV, the spectrum exhibits a small shoulder at around 285.4 eV that we will discuss in more detail below. For a more quantitative evaluation of the angular dependence shown in Fig. 2(a), the average molecular tilt angle β between the molecular long axis and the surface normal was determined. We applied the fitting procedure according to Eq. (1) introduced by Zheng *et al.*, which considers azimuthal anisotropy of the ordered domains inside the organic layer³⁰

$$\frac{I_V(\theta)}{I_V(\theta = 90^\circ)} = 1 + P \times \left(\frac{2}{\sin^2 \alpha} - 3 \right) \times \cos^2 \theta, \quad (1)$$

where θ is the photon incidence angle, P is the degree of polarization ($P = 0.91$ for the HE-SGM beamline), and α is the angle included by the direction of the final state orbital and the surface normal. For the analysis, we used the least-square fitted intensities of the low-energetic C1s $\rightarrow\pi^*$ (C=C) resonances, which are not affected by the C1s

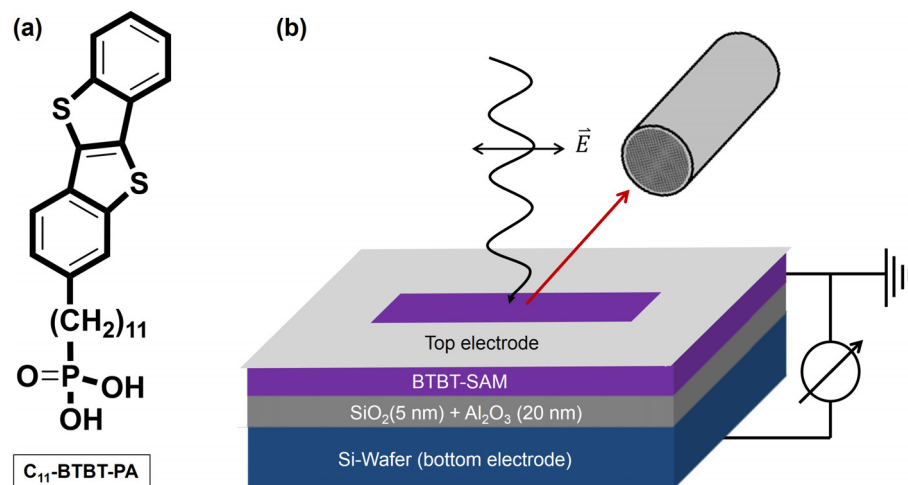


FIG. 1. (a) Chemical structure of BTBT-C11-PA from which the BTBT-SAM was prepared. (b) Scheme of the device setup and measurement geometry used for *in operando* studies of BTBT-SAMs. For an electrical contact, the sample is covered by a stainless steel top electrode with a 5 × 10 mm² window.

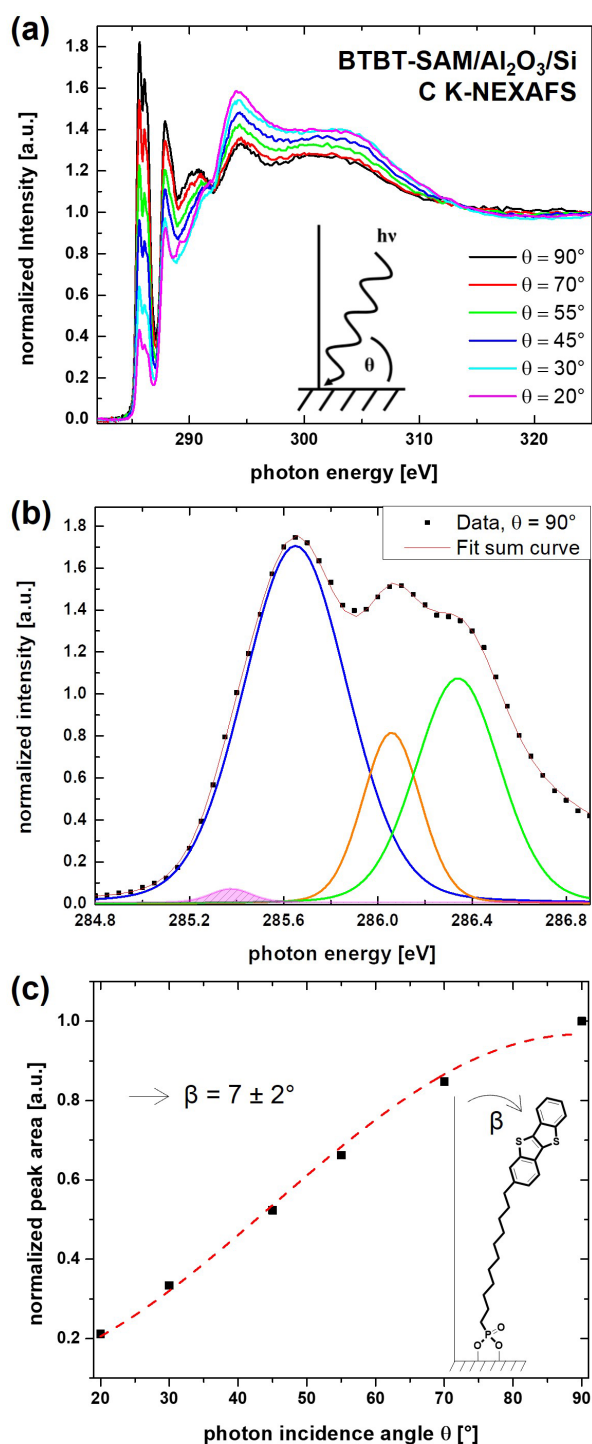


FIG. 2. (a) C K-edge NEXAFS of BTBT-SAMs recorded for different incident angles θ . (b) Magnification of the π^* -region with fitted absorption intensities at a photon incidence angle of $\theta = 90^\circ$. Peak assignments are given in the text. (c) Dependence of the integral absorption on the π^* -region at various incidence angles θ . The average molecular tilt angle β of the BTBT subunit is derived according to Eq. (1).

absorption threshold and, therefore, allow for an unambiguous evaluation of the average molecular tilt angle. The least-square fit of the integrated absorption intensities yields a molecular tilt angle $\beta = 90^\circ - \alpha$ of $\sim 7^\circ \pm 2^\circ$ [Fig. 2(c)]. This value is consistent with the expected (close to) upright standing confirmation reported in the literature as derived from x-ray reflectivity measurements in combination with molecular dynamics simulations.²⁵ Note, that the present analysis discusses the orientation of the BTBT core unit only since peak intensities assigned to the alkane subunit cannot be determined with sufficient accuracy as the peaks overlap with the absorption threshold.

Next we discuss the voltage or polarization effects observed in our NEXAFS study. Figure 3 summarizes the spectral modifications in the C1s NEXAFS for different gate voltages. As the BTBT-SAM is a low-voltage p-type material, the negative voltages (-3 , -5 V) correspond to the on-state, while the positive voltages ($+3$, $+5$ V) account for the off state.³¹ Owing to the close-to-perpendicular orientation of the molecules' substrate surface, the NEXAFS spectra were recorded at normal photon incidence ($\theta = 90^\circ$) where the C1s $\rightarrow \pi^*$ -transitions exhibit the highest intensity. To prevent potential beam damage, each NEXAFS spectrum was recorded on a fresh spot, and NEXAFS spectra without any applied voltage were compared before and after a series of voltage-dependent spectra. Neither line shape nor intensity modifications were discovered after recording a series of measurements for identical conditions.

Comparing NEXAFS spectra recorded in the on- and off-states displayed in Fig. 3(a), we found that the measured NEXAFS intensity is significantly reduced when a negative voltage was applied to the gate electrode, while we did not observe any spectral changes under positive bias. This effect can be seen across the whole energy range of the spectra, whereby it has the strongest effect in the π^* -region [Fig. 3(b)]. Apart from the overall intensity decrease, we observe a distinct increase in the shoulder at 285.4 eV [see Fig. 3(c) in comparison with Fig. 2(b)]. A more detailed evaluation of the voltage dependent spectra showed that the intensity of the underlying peak correlates with the applied gate voltage [Fig. 3(d)]. We must not forget to mention that the spectral modifications were no longer observed after the dielectric breakdown (voltages larger than ± 6 V), which is an unambiguous indication of a field-induced effect.

In the literature, several effects are discussed, which take place inside the organic layer and at the organic-semiconductor interface under an applied gate voltage. One potential effect, which could influence the NEXAFS intensities, is the change in the molecular orientation caused by alignment of the molecules inside the applied electric field. This was reported, e.g., for pentacene based OFETs, where an irreversible structural modification (i.e., decrease in d-spacing) was revealed using Raman spectroscopy.³² As the observed effects in our experiments are fully reversible and, in addition, the intensities for π^* - and σ^* -resonances decrease simultaneously for negative voltages, structural (orientational) modifications can be ruled out. Potential other effects could be field-induced molecular polarizations or a chemical shift corresponding to a band-bending like distortion of the electronic states.¹⁷ Molecular polarization is expected to modify the intensities and/or shift the energy levels independent from the polarity of the applied electric field. In contrast, a band-bending like effect at the interface would result in an antisymmetric change with respect to the applied gate voltage.¹⁶ Both effects were not observed in our experiments.

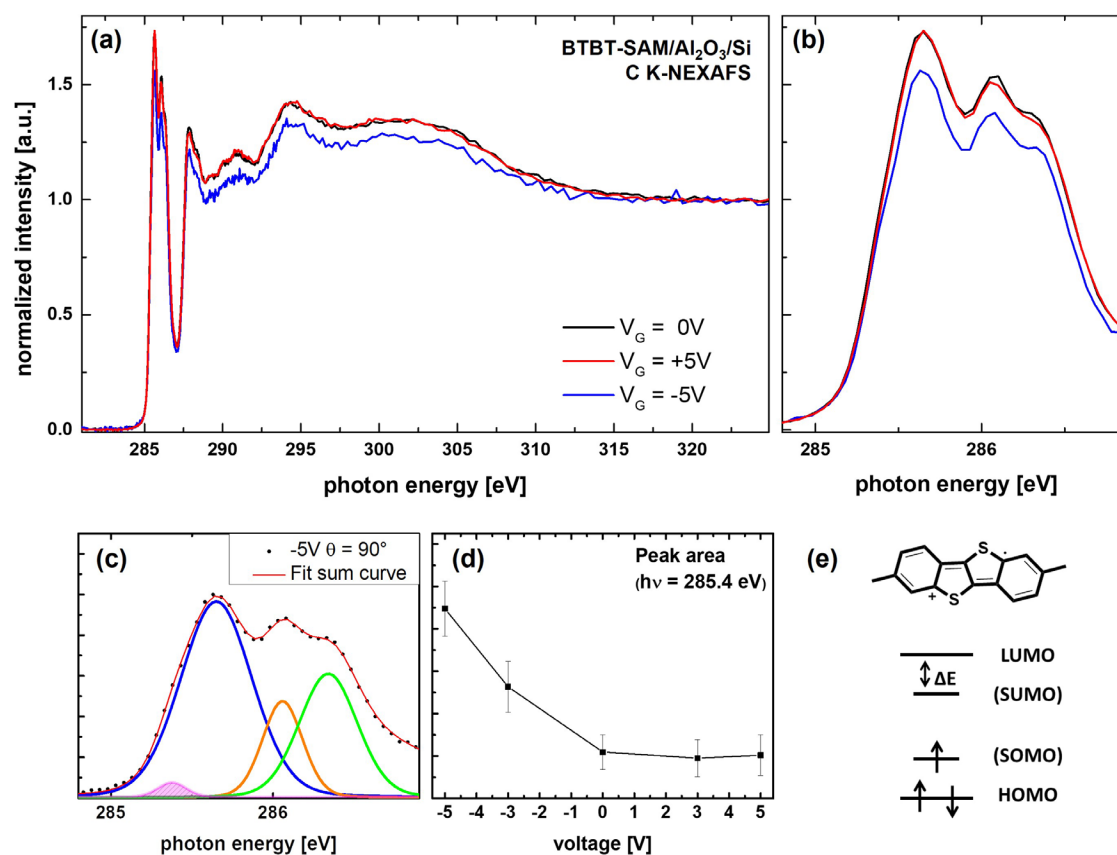


FIG. 3. (a) Gate-voltage dependent C K-edge NEXAFS spectra of BTBT-SAMs recorded at normal photon incidence and (b) corresponding expanded π^* -region. (c) Magnified π^* -region with fitted absorption intensities recorded at -5 V. (d) Gate-voltage dependence of the peak area for the resonance at 285.4 eV. (e) Chemical structure of a positively charged polaron on a BTBT core unit and corresponding energy diagram with ΔE being the energy between a neutral and a charged state.

Since BTBT is an organic p-type semiconductor and spectral modifications are observed for negative gate voltages only, the reason behind is rather given by a discontinuous phenomenon such as charge carrier accumulation. A variation in the gate voltage shows small but reproducible intensity variations of the low-energy resonance detected at 285.4 eV. The appearance of this resonance besides the $C1s \rightarrow LUMO$ transitions (π^* -resonances) indicates the presence of an additional unoccupied electronic state. It is well established that in organic semiconductors, a variety of sources, e.g., molecular disorder, defects, chemical impurities, or environmental effects, will lead to the formation of trap states and, therefore, localized charges at the dielectric/organic interface.³³ In conjugated systems, such charges are stored in the form of polarons, which can be considered as local deformations associated with gap states in between the HOMO and LUMO levels of the organic semiconductor [singly occupied/unoccupied molecular orbitals (SOMO/SUMO)], respectively, depicted in Fig. 3(e).^{12,34–36} The changes in energy between neutral and charged states is described as the polaron binding energy E_p caused by structural deformations.³⁷ For polythiophene chains, E_p is reported around 0.2 – 0.3 eV, which is in very good agreement with the energy difference ΔE between the shoulder at 285.4 eV and the first π^* -resonance at 285.7 eV.^{12,35} We, therefore, attribute the underlying peak at 285.4 eV to polaron-like

unoccupied states caused by the presence of charged species inside the organic layer or at the dielectric/organic interface. The gradual increase in the polaronic contribution at 285.4 eV upon negative gate voltage [Fig. 3(d)] can be assigned to the injection of field-induced charge carriers stored in polaronic states, which has been observed by other spectroscopic techniques as well.^{6,10,13,19,38} We, therefore, interpret our findings as the formation of a field-induced charge accumulation layer, in which the thickness and charge density are dependent on the strength of the applied electric field.^{10,34}

In K-edge NEXAFS, the measured intensity is correlated with the probability for an electronic transition, which is strongly dependent on the direction of the electric field vector of the incident linearly polarized light with respect to the final state orbital. The polaronic induced polarization, hence, impacts the transition probability, which can be seen as a modification, in our case a decrease in the spectral intensity. The strongest geometrical distortions are expected for electrical states residing inside the π -conjugated system, where the charge is localized.³⁴ Furthermore, the newly formed polaronic states arise from occupied HOMO- as well as unoccupied LUMO-states and, therefore, result in an additional decrease in the density of unoccupied states.¹³

Finally, we like to address the question why previous NEXAFS studies on BTBT-derivatives did not probe polaronic states.^{26,29}

Conventional electron spectroscopic studies use film thicknesses in the range of several organic layers and, thus, do not offer direct access to the dielectric/organic interface without interfering absorption (or signals) from the unaffected organic semiconductor bulk material. In particular, the overall low density of polarons makes it even more difficult to detect this electronic state in multilayer samples.

In summary, we have investigated field-induced electronic state modifications in p-type organic materials by near-edge x-ray absorption fine structure spectroscopy. To avoid interferential absorption from the bulk, we used an ultimately thin BTBT-based self-assembled monolayer as an active layer material in an OFET-type setup. In contrast to previously reported NEXAFS studies on BTBT-derivatives, we reproducibly observed a small shoulder at energies below the first π^* -resonance, in which we attribute to polaronic states caused by charged species at the dielectric/organic interface. When a negative voltage was applied to the back gate electrode, the overall intensity decreased, while no changes were determined for positive gate voltages. The effect was found to be most pronounced in the π^* -region. Furthermore, the polaronic peak increased as a function of the applied gate voltage. These results suggest that the modifications in core-excitation spectra can be attributed to field-induced charges of polaronic nature and fall in line with previous findings in the literature using optical spectroscopy.

The Helmholtz-Zentrum für Materialien und Energie (Berlin, Germany) is gratefully acknowledged for beamtime allocation, technical assistance, and travel support. Dr. M. Jank (Fraunhofer IISB, Erlangen) provided the ALD-AlO_x substrates. Financial support by the German Research Foundation (DFG) via the Research Training Group GRK 1896 “*In situ* microscopy with electrons, x-rays and scanning probes,” Project ID 182849149-SFB 953, the Federal Ministry of Education and Research (BMBF Project No. 05K19WE2), and the “Solar technologies go hybrid (SolTech)” initiative by the State of Bavaria is gratefully acknowledged. Baolin Zhao (No. 201706060215) thanks the support from the China Scholarship Council (CSC). We would like to thank Professor T. Clark and Professor D. M. Guldi for fruitful discussions.

AUTHOR DECLARATIONS

Conflict of Interest

The authors have no conflicts to disclose.

Author Contributions

Manuel Johnson: Formal analysis (equal); Funding acquisition (equal); Investigation (equal); Project administration (equal); Supervision (equal); Validation (equal); Visualization (lead); Writing – original draft (equal); Writing – review & editing (equal). **Tim Hawly:** Formal analysis (equal); Investigation (equal); Validation (equal); Visualization (equal); Writing – original draft (equal); Writing – review & editing (equal). **Baolin Zhao:** Formal analysis (equal); Investigation (supporting); Validation (supporting); Writing – original draft (supporting); Writing – review & editing (equal). **Marcus Halik:** Formal analysis (supporting); Investigation (supporting); Validation (supporting); Visualization (supporting); Writing – original draft (supporting). **Alexei Nefedov:** Formal analysis (equal); Investigation (equal); Validation (equal); Writing – original draft (equal); Writing – review & editing (equal). **Rainer H Fink:** Formal analysis (equal);

Funding acquisition (equal); Investigation (equal); Project administration (equal); Supervision (equal); Validation (equal); Writing – original draft (equal); Writing – review & editing (equal).

DATA AVAILABILITY

The data that support the findings of this study are available from the corresponding author upon reasonable request.

REFERENCES

- ¹M. Mas-Torrent and C. Rovira, *Chem. Soc. Rev.* **37**(4), 827 (2008).
- ²H. Minemawari, T. Yamada, H. Matsui, J. Tsutsumi, S. Haas, R. Chiba, R. Kumai, and T. Hasegawa, *Nature* **475**(7356), 364 (2011).
- ³Y. Diao, B. C. Tee, G. Giri, J. Xu, D. H. Kim, H. A. Becerril, R. M. Stoltenberg, T. H. Lee, G. Xue, and S. C. Mannsfeld, *Nat. Mater.* **12**(7), 665 (2013).
- ⁴Z. Lin, X. Guo, L. Zhou, C. Zhang, J. Chang, J. Wu, and J. Zhang, *Org. Electron.* **54**, 80 (2018).
- ⁵Q. Wang, F. Yang, Y. Zhang, M. Chen, X. Zhang, S. Lei, R. Li, and W. Hu, *J. Am. Chem. Soc.* **140**(16), 5339 (2018).
- ⁶H. Sirringhaus, *Adv. Mater.* **26**(9), 1319 (2014).
- ⁷M. Muccini, *Nat. Mater.* **5**(8), 605 (2006).
- ⁸Y. Chen, B. Lee, H. T. Yi, S. S. Lee, M. M. Payne, S. Pola, C.-H. Kuo, Y.-L. Loo, J. E. Anthony, and Y. T. Tao, *Phys. Chem. Chem. Phys.* **14**(41), 14142 (2012).
- ⁹B. Rösner, N. Zeilmann, U. Schmidt, and R. H. Fink, *Org. Electron.* **15**(2), 435 (2014).
- ¹⁰Z. Q. Li, G. M. Wang, N. Sai, D. Moses, M. C. Martin, M. Di Ventra, A. J. Heeger, and D. N. Basov, *Nano Lett.* **6**(2), 224 (2006).
- ¹¹P. J. Brown, H. Sirringhaus, M. Harrison, M. Shkunov, and R. H. Friend, *Phys. Rev. B* **63**(12), 125204 (2001).
- ¹²K. E. Ziemelis, A. T. Hussain, D. D. C. Bradley, R. H. Friend, J. Rühle, and G. Wegner, *Phys. Rev. Lett.* **66**(17), 2231 (1991).
- ¹³J. H. Burroughes, C. A. Jones, and R. H. Friend, *Nature* **335**(6186), 137 (1988).
- ¹⁴H. Sirringhaus, *Adv. Mater.* **17**(20), 2411 (2005).
- ¹⁵C. Hub, M. Burkhart, M. Halik, G. Tzvetkov, and R. Fink, *J. Mater. Chem.* **20**(23), 4884 (2010).
- ¹⁶H. S. Kato, H. Yamane, N. Kosugi, and M. Kawai, *Phys. Rev. Lett.* **107**(14), 147401 (2011).
- ¹⁷N. Nagamura, Y. Kitada, J. Tsurumi, H. Matsui, K. Horiba, I. Honma, J. Takeya, and M. Oshima, *Appl. Phys. Lett.* **106**(25), 251604 (2015).
- ¹⁸G. Horowitz, *J. Mater. Res.* **19**(7), 1946 (2004).
- ¹⁹S. Jiang, Q. Wang, J. Qian, J. Guo, Y. Duan, H. Wang, Y. Shi, and Y. Li, *ACS Appl. Mater. Interfaces* **12**(23), 26267 (2020).
- ²⁰E. C. Smits, S. G. Mathijssen, P. A. Van Hal, S. Setayesh, T. C. Geuns, K. A. Mutsaers, E. Cantatore, H. J. Wondergem, O. Werzer, and R. Resel, *Nature* **455**(7215), 956 (2008).
- ²¹D. O. Hutchins, O. Acton, T. Weidner, N. Cernetic, J. E. Baio, G. Ting, D. G. Castner, H. Ma, and A. K.-Y. Jen, *Org. Electron.* **13**(3), 464 (2012).
- ²²A. V. Parry, K. Lu, D. J. Tate, B. Urasinska-Wojcik, D. Caras-Quintero, L. A. Majewski, and M. L. Turner, *Adv. Funct. Mater.* **24**(42), 6677 (2014).
- ²³C. D. Heinrich, P. M. Reichstein, and M. Thelakkt, *ACS Appl. Mater. Interfaces* **10**(41), 35441 (2018).
- ²⁴J. Stöhr, *NEXAFS Spectroscopy* (Springer Science & Business Media, 2013).
- ²⁵T. Schmaltz, B. Gothe, A. Krause, S. Leitherer, H. G. Steinruck, M. Thoss, T. Clark, and M. Halik, *ACS Nano* **11**(9), 8747 (2017).
- ²⁶H. Watanuki, K. Mitsuhashi, and M. Takizawa, *e-J. Surf. Sci. Nanotechnol.* **16**, 79 (2018).
- ²⁷J. Kikuma and B. P. Tonner, *J. Electron Spectrosc. Relat. Phenom.* **82**(1–2), 53 (1996).
- ²⁸J. Stöhr, J. L. Gland, E. B. Kollin, R. J. Koestner, A. L. Johnson, E. L. Muettterties, and F. Sette, *Phys. Rev. Lett.* **53**(22), 2161 (1984).
- ²⁹T. Hawly, M. Johnson, A. Späth, H. Nickles Jäkel, M. Wu, E. Spiecker, B. Watts, A. Nefedov, and R. H. Fink, *ACS Appl. Mater. Interfaces* **14**(14), 16830 (2022).
- ³⁰F. Zheng, B.-N. Park, S. Seo, P. G. Evans, and F. J. Himpsel, *J. Chem. Phys.* **126**(15), 154702 (2007).

- ³¹T. Schmaltz, A. Y. Amin, A. Khassanov, T. Meyer-Friedrichsen, H. Steinrück, A. Magerl, J. J. Segura, K. Voitchovsky, F. Stellacci, and M. Halik, *Adv. Mater.* **25**(32), 4511 (2013).
- ³²H.-L. Cheng, W.-Y. Chou, C.-W. Kuo, Y.-W. Wang, Y.-S. Mai, F.-C. Tang, and S.-W. Chu, *Adv. Funct. Mater.* **18**(2), 285 (2008).
- ³³H. F. Haneef, A. M. Zeidell, and O. D. Jurchescu, *J. Mater. Chem. C* **8**(3), 759 (2020).
- ³⁴G. Horowitz, *Adv. Mater.* **10**(5), 365 (1998).
- ³⁵H. Sirringhaus, P. J. Brown, R. H. Friend, M. M. Nielsen, K. Bechgaard, B. M. W. Langeveld-Voss, A. J. H. Spiering, R. A. Janssen, E. W. Meijer, and P. Herwig, *Nature* **401**(6754), 685 (1999).
- ³⁶L. Yuan, C. Franco, N. Crivillers, M. Mas-Torrent, L. Cao, C. S. S. Sangeth, C. Rovira, J. Veciana, and C. A. Nijhuis, *Nat. Commun.* **7**(1), 12066 (2016).
- ³⁷B. Hanulikova and I. Kuritka, *J. Mol. Model.* **20**(10), 2442 (2014).
- ³⁸P. Kappen, P. S. Hale, N. Brack, W. Prissanaroon, and P. J. Pigram, *Appl. Surf. Sci.* **253**(3), 1473 (2006).